Journal of Geodetic Science

• 1(1) • 2011 • 52-58 DOI: 10.2478/v10156-010-0007-2 •

Orientation of the Geometrically Best fitting Triaxial Lunar Ellipsoid with Respect to the Mean Earth/Polar Axis Reference Frame

Research Article

H. Bâki Iz[1]*, C.K. Shum[2], X.L. Ding[1], C.L. Dai[2]

1 Dept. of Land Surveying and Geo-Informatics, The Hong Kong Polytechnic University, Hong Kong, China
2 Division of Geodetic Science, School of Earth Sciences, The Ohio State University, USA

Abstract:

This study provides new estimates for the orientation of a geometrically best fitting lunar triaxial ellipsoid with respect to the mean Earth/polar axis reference frame calculated from the footprint positions of the Chang'E-1 (CE-1), SELenological and ENgineering Explorer (SELENE) laser altimetry measurements and Unified Lunar Control Networks 2005, (ULCN 2005) station coordinates. The semi-principal axes of the triaxial ellipsoid and the coordinates of its geometric center are also calculated simultaneously. All the estimated parameters from all three data sets are found to be consistent. In particular, the RMS differences of the semi-principal axes of the triaxial ellipsoids and the locations of their geometric centers from solutions with and without modeling Euler angles (orientation of the triaxial ellipsoid) using uniformly distributed laser altimetry (LAL) footprints are 29 and 31 m respectively. The misclosures of all the solutions indicate a better fit for the triaxial ellipsoid to the footprint and station coordinates if the Euler angles are included in the models.

Keywords:

Euler angles • lunar figure • lunar laser altimetry • lunar orientation • Chang'E-1 • SELENE • ULCN 2005

Received 24 November 2010; accepted 30 November 2010

1. Introduction

The parameters of various lunar figures are of interest to the scientific community working on lunar exploration. Improved quantification of the geometric and dynamic figure of the Moon allows one to study the origin of the Moon, its interior structure, and composition. A mathematical reference surface is also required for horizontal lunar control networks for lunar mapping as in the case of the Earth. To achieve these ends, improved estimates of the size of the lunar figures, and their geometric centers (center of figure) with respect to the center of mass of the Moon, are needed.

In 2009, Iz published the most recent semi-principal axes of a triaxial ellipsoid and its geometric center, at that time, using a geometric model of a triaxial ellipsoid from the ULCN lunar control station positions (Archinal et al., 2005). Since then, two of the recent lunar missions, namely, Chang'E-1 (China) and SELENE (Japan), where a major goal has been to map the surface of the Moon, produced over 17 million laser altimetry (LAL) measurements of the lunar surface. Most recently, Ping (2009) and Araki (2009) estimated the semi-principal axes of a triaxial ellipsoid from the spherical harmonic models of the lunar topography derived from the Chang'E-1 (CE-1) and SELENE LAL data. Iz et al. (2010b) updated these estimates using the footprint coordinates of the LAL measurements from the CE-1 and SELENE missions for spherical, biaxial, and triaxial ellipsoidal representations of the lunar figure. In all these solutions, the principal axes of the lunar figures were assumed to be parallel to the axes of the mean Earth/polar axis reference frame but their geometric centers were allowed to get adjusted with respect to the origin of the reference frame, which coincides with the center

*E-mail: lshbiz@polyu.edu.hk

VERSITA

of mass of the Moon. An earlier solution by Smith et al. (1996) using Clementine mission's LAL measurement revealed that the polar axis of the triaxial lunar ellipsoid is tilted toward the Earth by 24 degrees in the mean Earth / polar axis reference frame, evidently caused by the uneven distribution of large lunar topographical features, mainly South Pole-Aitken basin (ibid).

This study provides new estimates for the orientation parameters of the lunar triaxial ellipsoid (Euler angles), solved together with the shape parameters of the triaxial ellipsoid (its semi-principal axes) and the position of its geometric center with respect to the mean Earth/polar axis reference frame using three contemporary data sets; ULCN 2005 station coordinates, and CE-1and SELENE LAL footprint positions.

2. Data Sources

ULCN 2005 is a unified three dimensional photogrammetrically determined network, which consists of 272,931 control points realized in the mean Earth/polar axis reference system with an average of one point approximately 46 km^2 (Archinal et al., 2005). The accuracy of the ULCN 2005 control points is reported to be a few hundred meters (Iz et al. 2009).

CE-1 is the first lunar exploration mission of China, which was launched on October 24th 2007. The onboard LAL system produced measurements with a surface spot size of 120 m when satellite altitude was about 200 km. The distance/ranging resolution of LAL measurements was estimated to be less than $\pm$5 m (Ping et al. 2009). The along-track shot spacing was about 1.4 km, and the minimum foot spacing along the equator is about 7.5 km after two months of measurements. In this study, over 8.5 million selenocentric distances (after removing over 300,000 outliers) and their latitudes and longitudes of CE-1 LAL measurements' footprints, provided by the China Lunar Exploration Center are used. The radial distances of the LAL footprints were calibrated by comparing them against the radial distances of the Lunar Laser Ranging (LLR) sites (Iz, et al. 2010b).

Japan Aerospace Exploration Agency (JAXA) launched SELENE on 14 September 2007. The main satellite KAGUYA, orbited the Moon 100 km $\pm$30 km above the lunar surface with an inclination of 90$\pm$1 degrees and a period of two hours. The footprint size of the laser spot produced by the onboard LAL system was typically 40 m, and the data spacing is about 1.6 km in along-track direction. The range resolution was 1 m with 5 m accuracy (Araki et al. 2009). JAXA (2009) provided over 8.8 million selenocentric SELENE LAL measurements and their subsatellite locations (latitudes and longitudes of the LAL measurement footprints). Statistical analysis of the LAL footprint positions nearby the LLR station coordinates did not show any statistically significant differences (ibid), hence no calibration correction was applied to the SELENE LAL footprint radial distances.

3. Mathematical and Statistical Models

Earlier approaches in computing the orientation of the lunar figure involved spherical harmonic models of the lunar topography. Through the analysis of their spherical harmonic coefficients, the lunar orientation parameters were estimated (Smith et al. 1996). Alternatively, as early as 1968, Gavrilov used the least squares method, to estimate the coefficients of an ellipsoidal quadric from which he calculated the lunar orientation parameters using the eigenvectors of the estimated coefficients of the quadric. What is common to both approaches is that the orientation angles are estimated using a two-step procedure. In this study, a direct formulation is developed, which is equivalent to the second approach under proper conditions.

Consider the following representation of the lunar shape by a triaxial ellipsoid whose equatorial semi-major axis is denoted by a, semi-minor axis by b, and polar axis by c. The coordinates of its geometric center in the mean Earth/polar axis reference frame, are denoted by x_c, y_c, z_c. The triaxial ellipsoid's orientation with respect to the x, y, z axes of the mean Earth/polar axis reference system (whose origin is at the center of mass of the Moon) is given by the three Eulerian angles α, β, and γ respectively;

$$\begin{bmatrix} x-x_c \\ y-y_c \\ z-z_c \end{bmatrix}^T \mathbf{R}^T \begin{bmatrix} a^{-2} & 0 & 0 \\ 0 & b^{-2} & 0 \\ 0 & 0 & c^{-2} \end{bmatrix} \mathbf{R} \begin{bmatrix} x-x_c \\ y-y_c \\ z-z_c \end{bmatrix} - 1 = 0 \tag{1}$$

where,

$$\mathbf{R} := \begin{bmatrix} 1 & 0 & 0 \\ 0 & \cos\alpha & \sin\alpha \\ 0 & -\sin\alpha & \sin\alpha \end{bmatrix} \begin{bmatrix} \cos\beta & 0 & -\sin\beta \\ 0 & 1 & 0 \\ \sin\alpha & 0 & \cos\beta \end{bmatrix} \begin{bmatrix} \cos\gamma & \sin\gamma & 0 \\ -\sin\gamma & \cos\gamma & 0 \\ 0 & 0 & 1 \end{bmatrix}. \tag{2}$$

In the statistical context, this is a non-linear conditioned equations with unknown parameters, which contain the Cartesian coordinates x, y, z, that refer to the locations of the laser altimetry footprints (as observations) to be adjusted, and the semi-principal axes of the triaxial ellipsoid (a, b, c), and its geometric center (x_c, y_c, z_c), are the unknown parameters to be estimated.

As far as the statistical properties of the Cartesian coordinate components of the footprints are concerned, their standard errors are assumed to be the same and not correlated with each other (i.e. the weight matrix is equal to identity). Note that, the standard errors of the estimates may need to be scaled by the a posteriori variance of unit weight (variance factor) after the adjustment. However, because the residuals always include unmodeled and non-stochastic lunar topography, the a priori variance of unit weight cannot be replaced by its a posteriori variance. Hence, a conservative 100 m standard error, a conservative estimate

inferred from a parallel study by Iz et al. (2010a), was assumed for each component of the CE-1 and the SELENE footprint Cartesian coordinate errors and an a priori variance of unit weight equal to one in evaluating the standard errors of the estimates. The above condition equations with unknown parameters are solved using the iterative algorithm given by Pope (1972), (cf. Iz, 2009 for a partitioned computational counterpart).

Two different solution scenarios were considered to assess the impact of modeling the orientation on the triaxial ellipsoid and the location of its geometric center. Under the first scenario, labeled, solutions without Euler angles, the lunar figure is represented by a triaxial ellipsoid whose semi-principal axes are parallel to the mean Earth/polar axis reference frame (i.e. Euler angles are set to zero), together with its geometric center. Alternative solutions, labeled solutions with Euler angles, included the three Eulerian angles in addition to the semi-principle axes and the coordinates of the geometric center of the triaxial ellipsoid to be estimated.

4. Solution Comparisons

Table 1 lists the estimated triaxial ellipsoid's shape and its geometric center parameters without considering its orientation in the solution model (without Euler angles) using different data sets. The standard errors of the estimates are less than 1 m for the semi-principal axes and the geometric center of the triaxial ellipsoid. The standard errors of all the estimates are found to be less than 10 m for the solution using ULCN 2005 station coordinates. The estimated parameters reported by Smith et al. (1996) that were calculated from the spherical harmonic models of the lunar topography using Clementine mission LAL measurements are also included in this table in order to establish a baseline for the solutions with and without triaxial ellipsoid orientation parameters. Note that this is the only recent solution for the orientation of a triaxial ellipsoid but unfortunately the geometric center of the triaxial ellipsoid was not modeled.

Two additional solutions using downsampled CE-1 and SELENE data are also reported because, initially, the solutions with the Euler angles using all the available data had convergence problems caused by the high density of the data at polar regions as a result of the polar orbits of the CE-1 and SELENE missions and the presence of multiple local minima in minimizing the target function of the least squares solution of the conditioned equations with unknown parameters. Instead of down weighting the LAL data at the polar regions, the LAL data from both missions were downsampled using randomly generated two sets of 250,000 uniformly distributed points on a unit sphere (Appendix A). Fortuitously, it turned out that, the global convergence for the nonlinear solutions with the lunar orientation parameters can also be achieved if the estimated parameters from solutions with the downsampled data are used as approximate values (nominal values) to start the iterations overcoming the convergence problem to the global minimum.

Table 1 results show that there are large differences in the semi-principal axes of the ellipsoids from Clementine (Smith et al., 1996) and the other solutions mainly because of the limited distribution of the LAL measurements (not available towards the poles) and the omission of the geometric center of triaxial ellipsoid parameters in the Clementine solution model.

As far as the differences of the estimated parameters among the remaining solutions are concerned, different solutions agree well with each other especially between the solutions with the downsampled data for which 48 m is the largest difference in the equatorial semi-major axes, and a minimum difference of 5 m in the polar axes, with 29 m RMS difference in the estimated parameters. Part of the improved agreement between the parameters of the solutions using the downsampled data can be attributed to the uniform distribution (in statistical sense) of the data used in the solutions (down-sampling also removes some of the erroneous CE-1 data at polar regions as will be discussed in the following paragraphs) and the successful calibration of the CE-1 data.

Table 2 lists the solutions with Euler angles. The standard errors of the estimated parameters are again less than 1 m for the lunar shape and for the center of the triaxial ellipsoid parameters and less than 0.001 degrees for the Euler angles. In all these solutions, the standard errors are more precision statements than representative of the accuracies of the estimated parameters because of the unmodeled lunar topography in the mathematical models. The latitudes and longitudes of the lunar North Pole (NP) position of the polar axis of the triaxial ellipsoid in the mean Earth/polar axis coordinate frame calculated from the estimated Euler angles are also included in this table. The Euler angles for the Clementine solution were not reported by Smith at al. (1996).

Some of the results are in better agreement across the solutions as revealed by the parameter differences from solutions with Euler angles. The differences in the estimated parameters in some cases can be as small as a few meters. Although the ULCN 2005 data are not completely independent from the Clementine LAL data (the latter is included in the former), CE-1 and SELENE LAL data are completely independent. These two data sets are the product of different instruments on board of the satellites at different altitudes, and processed by different software, yet producing measurements that enable solutions in some cases, which are in agreement down to 3 meters (in b and c, in Table 2).

Table 2 estimates also reveal that the CE-1 solutions using all available data deviate systematically from the other solutions significantly in the polar axis and the estimated x_c component of the geometric center of the triaxial ellipsoid. The closer agreement between the CE-1 and SELENE solutions estimates (29 m RMS difference) from the downsampled data suggests that the solutions that are based on all available data are influenced by the dense LAL data at the polar regions (near polar orbits) that are reduced in number after down-sampling. An earlier study by Shum et al. (2010) revealed large cross over differences in the CE-1 orbits over the poles thereby adversely influencing the solutions using all the available LAL data.

Table 1. Solutions *without* Euler angles. All units for all the estimates are in meters. The standard errors of the estimates are less than 1m for the semi-principal axes of the triaxial ellipsoids and the coordinates of their geometric centers based on 100 m a priori standard deviation in the Cartesian coordinates. The radial distances of the LAL footprints were calibrated at nearby LLR sites (Iz et al., 2010b). The Clementine solution did not include center of figure parameters (Smith et al., 1996). N/A: Not available. RMS refers to the RMS misclosures.

	Clementine*	ULCN 2005	CE-1 All Data	SELENE All Data	CE-1 Sampled	SELENE Sampled
a	1738056	1737899	1737810	1737953	1738022	1738070
b	1737843	1737570	1737597	1737594	1737615	1737661
c	1735485	1735742	1735947	1735996	1735686	1735691
x_c	0	-1658	-1485	-1671	-1718	-1736
y_c	0	-681	-695	-698	-710	-721
z_c	0	133	269	207	217	230
RMS	N/A	3507	3931	4528	3759	3786

*Smith et al., 1996.

Table 2. Solutions *with* Euler angles. The standard errors of the estimates for the semi-principal axes of the triaxial ellipsoids and the coordinates of their geometric centers are less than 1m and less than 0.001 degrees for the Euler angles based on 100 m a priori standard deviation in the Cartesian coordinates. The values listed in the last row are the latitudes and longitudes of the lunar North Pole (NP) position of the triaxial ellipsoid in the mean Earth/polar axis coordinate system.

	Clementine*	ULCN 2005	CE-1 All Data	SELENE All Data	CE-1 Sampled	SELENE Sampled
a	1739020	1739001	1739057	1739115	1739024	1739088
b	1737567	1737249	1737323	1737335	1737338	1737370
c	1734840	1734960	1734998	1735158	1734963	1734969
x_c	0	-1628	-1451	-1567	-1718	-1736
y_c	0	-695	-676	-686	-714	-723
z_c	0	182	262	205	220	226
α	N/A	19.200	18.75	19.18	17.530	17.390
β	N/A	21.620	25.52	23.75	21.350	21.240
γ	N/A	29.590	27.95	27.59	27.190	27.330
NP	66.00N 10.40E	61.440N 13.860W	58.750N 10.340W	59.870N 13.300W	62.690N 13.850W	62.850N 13.600W
RMS	N/A	3075	3077	2896	3367	3391

*Smith et al., 1996.

Meanwhile, there is a considerable difference in the orientation of the lunar figures, mainly between those from the Clementine solution and the others (NP values in Table 2). The Clementine data is also included in the ULCN 2005 solution, and their estimated semi-principal axes of triaxial ellipsoids are in close agreement; however, their NP positions are different suggesting that the difference in the orientation is likely due to the center of figure parameters not being included in the Clementine model. The global distribution of the Clementine data is also limited, not covering the North and South poles, as compared to the other data sets. In any case, the end point of the south polar axis still remains within the boundaries of the South Pole-Aitken basin in all other solutions demonstrating the dominant role played by this extraordinary topographical feature in the solutions. At this point, it is important to note that the prevalence of the South Pole-Aitken basin in the orientation of the triaxial ellipsoid in the Clementine solution evidence that the solutions from the coefficients of the spherical harmonic models of the lunar topography are not robust to the lunar topography as expected.

The RMS difference of the semi-principal axes of the triaxial ellipsoid and the estimates of its geometric center between the solutions using the downsampled CE-1 and SELENE data is 31 m; a solid performance of the downsampled data sets and a validation of the calibration for the CE-1 LAL radial footprints. The differences in the Euler angles estimated from the downsampled data sets are less than 4.3 km along the lunar equator. Evidently, the estimates for the Euler angles are more sensitive to the data sets when compared to the other parameters. This sensitivity is more due to the nature of the parameters (small variations in the angles lead to large displacements on the surface of the Moon) since the correlation matrix of the estimates for the downsampled data is nearly an identity matrix, exhibiting negligible correlations among the parameters.

The misclosures that are calculated using Equation (1) and (2) for

the different solutions are also informative (the RMS misclosures are listed in the last rows of Table 1 and 2). The misclosures were calculated using the estimated parameters and the observed footprint Cartesian coordinates, rather than the adjusted Cartesian coordinates which will result in zero misclosures if used. Although the misclosures are dominated by the differences between the radial distances of the footprints and the radial distances of their projected points on the ellipsoid (lunar topography), they are also influenced by the effect of errors in the horizontal LAL footprint positions, hence making them better statistics to assess the best fit.

The RMS misclosures (Table 2) from the solutions with Euler angles are consistently smaller compared to those from the solutions without Euler angles simply due to the freedom of the triaxial ellipsoid to orient itself in the solutions and the presence of large topographical features, mainly, South Pole-Aitken basin that dominate the orientation of the triaxial ellipsoids (Figure 1). Hence, it is evident that a triaxial ellipsoid representing the lunar shape, will not be aligned with the underlying lunar reference frame in these solutions. Note that the fit provided by the ULCN 2005 solution without the Euler angles is consistently smaller than the others. However, this is not the case for the solutions with the Euler angles for which the RMS misclosures of the solution with the downsampled SELENE data are improved by 10 percent over the RMS misclosures of the ULCN 2005 solution with Euler angles. Meanwhile, the RMS misclosures from the CE-1 and SELENE solutions with and without Euler angles both based on the downsampled data do not deviate much from each other (the difference in the RMS misclosures is only 2 m) when compared with the solutions with all data solutions RMS misclosures.

The consistent positive differences of the RMS misclosures with and without Euler angles, suggest that Euler angles must be included in the geometric model of a lunar figure, but unfortunately, we cannot support this conclusion statistically using a null-hypothesis test because of the presence of the unmodeled and non-stochastic lunar topography in the residuals, which makes all the statistical comparisons meaningless. Yet, the differences in the misclosures from without and with Euler angle solutions evaluated at each footprint locations and displayed in Figure 1 show unambiguously the impact of the inclusion of the Euler angles in the solutions, especially in the South Pole-Aitken basin region and on the highlands on the far side of the moon.

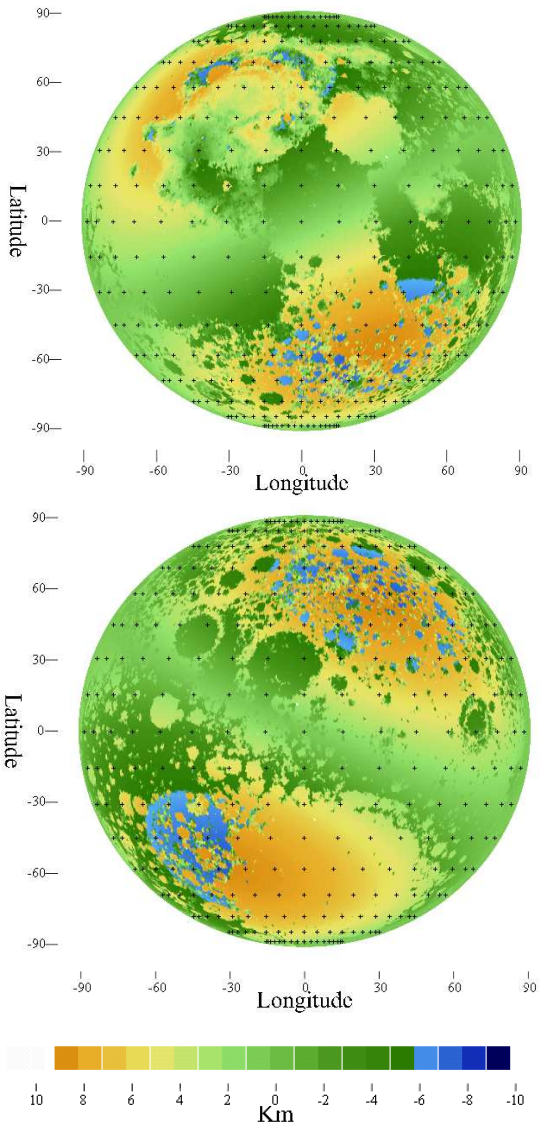

Figure 1. First, misclosures for solutions *with* and *without* Euler angles are calculated using Equation (2), as deviations from unity and scaled by 1737 km from the CE-1 down-sampled data. Their differences (*without* minus *with* Euler angles) for the near side (top) and far side are then plotted. The figure shows the locations and the magnitude of the changes in the misclosures as a result of considering Euler angles in the solution on an orthographic projection.

5. Conclusion

The lunar figure and center of figure parameters estimated from all three data sets, namely ULCN 2005, CE-1, and SELENE are consistent. In particular, the RMS differences between the estimated semi-principal axes of the triaxial ellipsoids and their locations are as small as 29 and 31 m for the solutions with and without Euler angles respectively, based on the downsampled LAL footprints from the CE-1 and SELENE missions over the lunar surface.

Meanwhile, smaller misclosures and better agreement between the solution parameters using the downsampled CE-1 and SELENE data suggest that CE-1 orbits above polar regions need further attention, possibly in modeling along-track satellite accelerations. The magnitudes of the estimated Euler angles and the differences in the misclosures between solutions with and without Euler angles confirm a better fit if the triaxial ellipsoid is allowed to adjust its orientation. The estimated location of the polar axis is

within the boundaries of the South Pole-Aitken basin in all solutions but deviates from the earlier Clementine solution in magnitude. It is also desirable to remove the contribution of the South Pole-Aitken basin, (the largest, deepest and oldest basin recognized on the Moon, and the biggest hole in the Solar System), in the solutions in order to better assess the shape and the orientation of the Moon. Nonetheless, additional runs with the Euler angles using an iteratively weighted scheme, where the weights are proportional to the topography to down-weight its influence, do not converge. Also, the solutions with the LAL data excluded from the South Pole-Aitken basin are ill-conditioned because of the poor geometry. The location of the pole axis of the triaxial ellipsoid (in the South Pole-Aitken basin region) inferred from the coefficients of the spherical harmonics of the lunar topography in an earlier solution shows that this approach is also unduly influenced by the lunar topography. It is therefore necessary to investigate and devise alternative models that are more robust to the effects of the large-scale lunar topography.

Appendix A

Two sets of 250,000 uniformly distributed points were generated on a lunar sphere, first by generating x, y, z independent standard normal variates, i.e., $\mathcal{N}(0,1)$, and then calculating

$$\left(\frac{x}{s} \quad \frac{y}{s} \quad \frac{z}{s} \right), \quad \text{where } s := \sqrt{x^2 + y^2 + z^2}$$

for each variate. The generated triplets are uniformly distributed on a sphere (Marsaglia, 1972). The random points were rescaled with an average radius of the Moon to generate uniformly distributed footprint positions on the lunar surface. Each lunar data set (CE-1 and SELENE) were then downsampled by choosing the nearest footprint for each uniformly distributed point.

Acknowledgement

This study was supported by the Hong Kong Polytechnic University grants G-U417 and 1-BB83. We gratefully acknowledge China Lunar Exploration Center and JAXA for providing us the CE-1 and the SELENE LAL data. Detailed comments by three anonymous reviewers improved the readability and presentation of the manuscript.

References

Araki H., Tazawa S., Noda H., Ishihara Y., Goossens S., Sasaki S., Kawano N., Kamiya I., Otake H., Oberst J., Shum C.K., (2009), Lunar Global Shape and Polar Topography Derived from Kaguya-LALT Laser Altimetry, Science Vol. 323, 898-900.

Araki H., Tazawa S., Noda H., Ishihara Y., Goossens S., Kawano N., Sasaki S., Kamiya I., Otake H., Oberst J., Shum C.K., (2009), The Lunar Global Topography by the Laser Altimeter (LALT) Onboard Kaguya (SELENE): Results from the One Year Observation, 40th Lunar and Planetary Science Conference, www.lpi.usra.edu/meetings/lpsc2009/pdf/1432.pdf

Archinal B.A., Rosiek M.R., Kirk R.L., Redding B.L., (2006), The Unified Lunar Control Network 2005: U.S. Geological Survey Open-File Report 2006-1367. http://pubs.usgs.gov/of/2006/1367/

Gavrilov I.V., (1968), The Geometric Figure and Dimensions of the Moon, Soviet Astronomy, AJ 12(2):319-325.

Iz H.B., (2009), New Parameters of Geometrically Best Fitting Lunar Figures, Journal of Applied Geodesy Vol. 3, 155-162.

Iz H.B., Chen Y.Q., King B.A., Ding X.L., Wu C., (2009), Deformation Analysis of the Unified Lunar Control Networks, Journal of Applied Geodesy, Vol. 3, 231-238.

Iz H.B., Chen Y.Q., Ding X.L., King B.A., Shum C.K., Wu C., Berber M., (2010a), Assessing Consistency of CE-1 and SELENE Reference Frames using Nearly-colocated Laser Altimetry Footprint Positions (under review).

Iz H.B., Shum C.K., Chen Y.Q., Dai C.L., (2010b), Improved Geometric Lunar Figure from CE-1 and SELENE Laser Altimetry (under review).

JAXA, https://www.soac.selene.isas.jaxa.jp/archive/index.html.en (2009).

Marsaglia G., (1972), Choosing a Point from the Surface of a Sphere, the Annals of Mathematical Statistics, Vol. 43(2):645-646.

Ping J., Heki H.K., Matsumoto K., Tamura Y., (2003), A Degree 180 Spherical Harmonic Model for the Lunar Topography, Adv. Space Res. Vol. 31(11):2377-2382.

Pope A.J., (1972), Some Pitfalls to be Avoided in the Iterative Adjustment of Nonlinear problems, Proc. 38th an. meet. Am. Soc. Phot.

Ping J., Huang Q., Shu R., Yan J., (2009), Lunar Topography Result from Chang'E-1 Laser Altimetry Mission, Presented at the 3rd

KAGUYA(SELENE) Science Working Team Meeting, Tokyo.

Shum C.K., Fok H., Yi Y., Araki H., Goossens S., Matsumoto K., Noda H., Ping J., Huang Q., Iz H.B., Chen Y., Williams J., (2010), Lunar Topography Model Refinement Combining Laser Altimetry from Lunar Orbiters The 4th Kaguya (SELENE) Science Working Team Meeting, Japan.

Smith D.E., Zuber M.T., Neumann G.A., Lemoine F.G., (1997), "Topography of the Moon from the Clementine LIDAR," JGR, 102, No. E1, 1591-1611.